WL-TR-91-4006

AD-A247 880

OXYGEN PERMEABILITY FOR SELECTED CERAMIC OXIDES IN THE RANGE 1200°C - 1700°C

E.L. Courtright
J.T. Prater
C.H. Henager
E.N. Greenwell
Pacific Northwest Laboratory
Richland, Washington 99352

May 1991

Final Report for Period September 1987 - May 1989

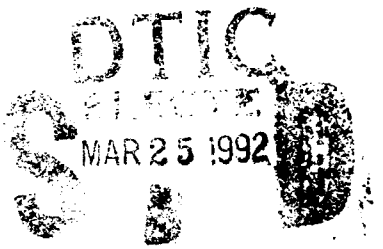

Approved for public release; distribution unlimited

MATERIALS DIRECTORATE
WRIGHT LABORATORY
AIR FORCE SYSTEMS COMMAND
WRIGHT-PATTERSON AIR FORCE BASE, OHIO 45433-6533

92-07610

NOTICE

When Government drawings, specifications, or other data are used for any purpose other than in connection with a definitely Government-related procurement, the United States Government incurs no responsibility or any obligation whatsoever. The fact that the government may have formulated or in any way supplied the said drawings, specifications, or other data, is not to be regarded by implication, or otherwise in any manner construed, as licensing the holder, or any other person or corporation; or as conveying any rights or permission to manufacture, use, or sell any patented invention that may in any way be related thereto.

This report is releasable to the National Technical Information Service (NTIS). At NTIS, it will be available to the general public, including foreign nations.

This technical report has been reviewed and is approved for publication.

ALLAN P. KATZ
Project Engineer

FOR THE COMMANDER

WALTER H. REIMANN, Chief
Materials Development Branch
Metals & Ceramics Division

If your address has changed, if you wish to be removed from our mailing list, or if the addressee is no longer employed by your organization, please notify WL/MLLM, WPAFB, OH 45433-6533 to help us maintain a current mailing list.

Copies of this report should not be returned unless return is required by security considerations, contractual obligations, or notice on a specific document.

UNCLASSIFIED

SECURITY CLASSIFICATION OF THIS PAGE

REPORT DOCUMENTATION PAGE

Form Approved OMB No. 0704-0188

1a. REPORT SECURITY CLASSIFICATION: Unclassified	1b. RESTRICTIVE MARKINGS
2a. SECURITY CLASSIFICATION AUTHORITY	3. DISTRIBUTION/AVAILABILITY OF REPORT: Approved for Public Release Distribution is Unlimited
2b. DECLASSIFICATION/DOWNGRADING SCHEDULE	
4. PERFORMING ORGANIZATION REPORT NUMBER(S)	5. MONITORING ORGANIZATION REPORT NUMBER(S): WL-TR-91-4006
6a. NAME OF PERFORMING ORGANIZATION: Pacific Northwest Laboratories; 6b. OFFICE SYMBOL (If applicable)	7a. NAME OF MONITORING ORGANIZATION: Materials Directorate Wright Laboratory
6c. ADDRESS (City, State, and ZIP Code): Richland, WA 99352	7b. ADDRESS (City, State, and ZIP Code): Wright-Patterson AFB, OH 45433-6533
8a. NAME OF FUNDING/SPONSORING ORGANIZATION: Wright Laboratory; 8b. OFFICE SYMBOL (If applicable): WL/MLLM	9. PROCUREMENT INSTRUMENT IDENTIFICATION NUMBER: FY 1457-87-N5054
8c. ADDRESS (City, State, and ZIP Code): Wright-Patterson AFB, OH 45433-6533	10. SOURCE OF FUNDING NUMBERS

PROGRAM ELEMENT NO.	PROJECT NO.	TASK NO.	WORK UNIT ACCESSION NO.
62102F	2420	01	01

11. TITLE (Include Security Classification)

Oxygen Permeability for Selected Ceramic Oxides in the Range 1200°C - 1700°C

12. PERSONAL AUTHOR(S)

E. L. Courtright, J. T. Prater, C. H. Henager, E. N. Greenwell

13a. TYPE OF REPORT	13b. TIME COVERED	14. DATE OF REPORT (Year, Month, Day)	15. PAGE COUNT
Final	FROM Sept.87 TO May 89	May 14, 1991	35

16. SUPPLEMENTARY NOTATION

17. COSATI CODES			18. SUBJECT TERMS (Continue on reverse if necessary and identify by block number)
FIELD	GROUP	SUB-GROUP	Oxygen permeability, ceramic oxides, coatings, high temperature materials

19. ABSTRACT (Continue on reverse if necessary and identify by block number)

Oxygen permeability as a function of temperature, was measured for several ceramic oxides over the range 1200°C-1700°C. Of the oxides tested, alumina, beryllia, yttria, lanthanum halfnate, and calcium zirconate exhibited the lowest permeabilities in order of decreasing resistance to oxygen transport. None of the permeability constants were less than the 10^{-10} to 10^{-12} gms O_2/cm·sec needed for a useful protective coating system above 1500°C. While oxygen permeability measurements on pure silica were not made during the course of this investigation, calculations indicate that silica is very impermeable to the diffusion of oxygen, with a permeability constant on the order of $2x10^{-12}$ gms O_2/cm·sec at 1700°C.

In some of the mixed oxide compounds, cation segregation was observed to occur with the more rapidly diffusing specie segregating to the side of highest oxygen potential. Thus, segregation must be considered when selecting mixed oxides for high temperature applications.

20. DISTRIBUTION/AVAILABILITY OF ABSTRACT	21. ABSTRACT SECURITY CLASSIFICATION
☐ UNCLASSIFIED/UNLIMITED ☐ SAME AS RPT ☒ DTIC USERS	Unclassified

22a. NAME OF RESPONSIBLE INDIVIDUAL	22b. TELEPHONE (Include Area Code)	22c. OFFICE SYMBOL
Allan Katz	(513) 255-9824	WL/MLLM

DD Form 1473, JUN 86 *Previous editions are obsolete.*

SECURITY CLASSIFICATION OF THIS PAGE

Unclassified

EXECUTIVE SUMMARY

Oxygen permeability as a function of temperature was measured for several ceramic oxides over the range 1200 to 1700°C. Of the oxides tested, alumina, beryllia, yttria, lanthanum halfnate, and calcium zirconate exhibited the lowest permeabilities in order of decreasing resistance to oxygen transport. None of the permeability constants were less than the 10^{-10} to 10^{-12} g O_2/cm·s needed for a useful protective coating system above 1500°C.

In some of the mixed oxide compounds, cation segregation was observed to occur with the more rapidly diffusing species segregating to the side of highest oxygen potential. Thus, segregation must be considered when selecting mixed oxides for high temperature applications.

While oxygen permeability measurements on pure silica were not made during the course of this investigation, calculations indicate that silica is very impermeable to the diffusion of oxygen, with a permeability constant on the order of 2×10^{-12} g O_2/cm·s at 1700°C. In practice, silicon-base coating systems have been successfully used to protect carbon/carbon composite materials for short exposures at this temperature, and molybdenum disilicide heating elements are being used for extended periods in high-temperature air furnaces.

Accession For
NTIS GRA&I ☑
DTIC TAB ☐
Unannounced ☐
Justification
By
Distribution/
Availability Codes
Dist | Special
A-1

ACKNOWLEDGMENTS

The authors wish to acknowledge the helpful assistance of Alon Graybeal who assembled the initial oxygen permeability measuring system and performed many of the preliminary scoping tests.

We also wish to thank Jeanne Biberstine for typing the original draft and for the able assistance of Wendy Bennett in preparing many of the key figures. Editorial assistance was provided by Darby Stapp and David Hilliard in preparing the final camera ready manuscript.

Funding support from the Air Force Materials Lab/Wright Research and Development Center is gratefully acknowledged together with the support and encouragement of Allan Katz, Project Monitor.

CONTENTS

FIGURES

TABLES

1.0 INTRODUCTION

Materials capable of withstanding high operating temperatures are needed for advanced propulsion systems, power generation equipment, and hypersonic flight applications. Candidates include refractory metals, intermetallics, ceramic-ceramic composites, and carbon/carbon composites. With the exception of some oxide compounds, all these materials are limited by poor oxidation resistance in the high-temperature operating regimes of interest. The principal method of overcoming this limitation has been to apply a protective coating to act as a barrier to oxygen permeability. In the case of refractory metals and intermetallic compounds, alloy additions have been useful in assisting the growth of protective oxide scales. Carbon/carbon composites are so sensitive to oxidation at high temperatures that complex coating systems together with internal and external sealants are required to ensure broad temperature range protection. The sealants form glasses which fill cracks and defects in the coating and prevent direct ingress of oxygen to the underlying substrate.

Many refractory oxides and oxide composite systems are thermodynamically stable in oxidizing environments. However, these materials typically do not have adequate strength, creep resistance, or the fracture toughness needed for high-temperature structural applications. If a high-strength nonoxide fiber, SiC or TiB_2 for example, is encapsulated in a protective oxide matrix, the permeability of oxygen through the matrix to the fiber interface may produce products that limit performance. For example, environmental degradation occurs in SiC whisker reinforced $Mg_2Al_2O_4$ upon exposure to air even though the components are thermodynamically stable under inert conditions [1]. Thus, protective fiber coatings are needed to enable the development of composite materials that otherwise would exhibit thermodynamic or environmental instability at high temperatures, and the search for refractory ceramic oxides with a high degree of thermo-oxidative stability and low permeability to oxygen continues to be an important part of developing material systems for high-temperature applications.

The primary objective of this research was to measure oxygen permeability in selected oxides and oxide compounds that appear to have potential for use as protective coatings or as barriers to oxygen diffusion in high-temperature structural materials.

2.0 BACKGROUND

If we consider the case of uni-directional diffusion under conditions of constant temperature and constant pressure, transfer of oxygen will occur in such a way as to reduce the chemical potential gradient. This can be defined mathematically by Fick's first law, which establishes that the particle flux through a plane of unit area is proportional to its concentration gradient:

$$J = P = -D\ \delta C/\delta x \qquad (1)$$

where C is the concentration per unit volume, x is the direction of diffusion, J and P are the flux or permeability defined in equivalent units per unit time per unit area, and D is the diffusion coefficient. The concentration gradient, $\delta C/\delta X$, is often unknown, and since D is not necessarily independent of C, direct permeability measurements can differ from diffusivity measurements made with the use of isotopic tracers.

If the concentration gradient is fixed by the oxygen partial at pressure P_1 on one side of a thin membrane (e.g. coating) and some lower pressure P_2 on the other side, permeation will occur at a constant rate. The concentration in the solid at the interface is a function of its solubility, which is proportional to P^n where n can be 1/2, 1/4, 1/6 depending upon the type of defect interactions. Thus,

$$P = -D\ \frac{\delta C}{\delta x} = -\frac{Db}{x}\ (P_1^n - P_2^n) \qquad (2)$$

where x is the membrane thickness, and b a constant. The permeability values reported in this report are expressed as the permeability constant (P•x), which is the permeability normalized for unit thickness.

A few simple calculations are shown in Figure 2.1 to illustrate the range of permeability constants required for various service applications. These calculations assume one-dimensional diffusion of oxygen through a coating of given thickness and complete reaction with the substrate. It is

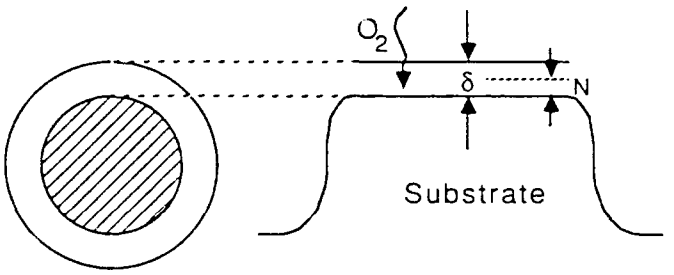

$$/ J_{O_2} / = \frac{D_{O_2} \cdot C_{O_2}}{\delta} \left(\frac{\text{moles } O_2}{\text{cm}^2 \cdot \text{sec}} \right) = \frac{dN}{dT} \frac{1}{\overline{V}_{\text{substrate}}} \times \frac{\text{moles } O_2}{\text{moles substrate}}$$

$$O_2 + M \rightarrow MO_2$$

For Coating $\delta = 1\mu$

$$\left(\frac{g\ O_2}{cm \cdot sec} \right)^*$$

Allowable Reaction dN (μ)	Time (h) 10	100	1000	10,000
1	10^{-12}	10^{-13}	10^{-14}	10^{-15}
10	10^{-11}	10^{-12}	10^{-13}	10^{-14}
100	10^{-10}	10^{-11}	10^{-12}	10^{-13}
1000	10^{-9}	10^{-10}	10^{-11}	10^{-12}

FIGURE 2.1. Approximate Minimum Permeability Requirements as a Function of Allowable Reaction Thickness. *Permeability constant - multiply by ten for each additional 10 μm of coating thickness.

further assumed that one mole of diatomic oxygen forms one mole of reaction product (MO_2), and no credit is taken for a reduction in permeability when the oxide scale thickens, which makes the assumption conservative.

If we were to have a 1-μm-thick barrier, as might be used to protect a ceramic fiber, and propose a reaction limit of 1 μm, the permeability constant (P•x) would have to be about 10^{-13} g O_2/cm/s to prevent the reaction zone from being consumed in 100 h. If the barrier was 100 μm in thickness, which is

more realistic of a protective coating system applied to a structural component, and our allowable reaction was 100 μm (4 mils), then the permeability would need to be about 10^{-10} g O_2/cm/s to achieve a 1000-h life time. For extended life applications (>1000 h), permeability constants less than 10^{-12} g O_2/cm/s will probably be required.

3.0 EXPERIMENTAL APPROACH

3.1 MATERIAL SELECTION

There are a number of possible mechanisms that explain atomic movement in crystalline oxides. Mobility by means of vacancies is likely the most common process in ionically bonded oxides. The most prevalent defect will be either vacancy pairs (Schottky defect) or vacancy-interstitial pairs (Frenkel defect). Even exactly stoichiometric oxides will contain some point defects. When aliovalent impurities are added to occupy interstial or substitutional positions in the lattice, the defect concentrations are increased and diffusion is generally enhanced.

For oxides with a fluorite lattice structure (ZrO_2, HfO_2, ThO_2), additions of divalent or trivalent cations are used to stabilize the structure. In this case, the concentration of oxygen ion vacancies are somewhat fixed by composition and are not so strongly temperature dependent [2]. Consequently, the oxygen ion diffusion coefficient has a temperature dependence that is fixed by the activation energy required for oxygen ion mobility. In general, it is hard to predict whether the temperature-dependent diffusion behavior of an oxide system will be intrinsic or impurity related. Thus, no doping studies were included in this work to examine the effects of defect interactions.

Instead, oxides with different crystal structures were selected and the oxygen permeability as a function of temperature experimentally determined. It was anticipated that the dense hexagonal close packed corundum and bixbyite lattices (e.g. Al_2O_3 Y_2O_3) would exhibit lower permeabilities than the more open fluorite lattices, but relative magnitudes need to be experimentally established.

The oxides and their associated crystal structures are given in Table 3.1. Process histories and summaries of the analytical characterization are also included.

TABLE 3.1. Materials History

Chemical Analysis Major Impurities				Process History				
Oxide	Source	wt%	Crystal Structure	Method	Temp (°C)	Time (Min)	Density gm/cc (% TD)	Xrd Analysis
Al_2O_3	Coors	>99.0 (Mfg Analysis)	Corundum (Hex CP)	Sintered	--	--	3.82 (98%)	
BeO	Brush Wellman	>99.5 (Mfg Analysis)	Wurtzite (Hex CP)	Sintered	--	--	2.85 (95%)	
$CaZrO_3$	Cerac	0.12 Si, 0.1 Al 0.08 Mg, 0.08 Na	Perovskite/Orthorhombic	HP[a]	1680	10	4.6 (98%)	Orthorhombic $CaZrO_3$
HfO_2 $10Y_2O_3$	PNL		Flourite (Cubic)	HP	2000	40	9.3 (98%)	Cubic HfO_2
HfO_2 $10Y_2O_3$ $3SiO_2$	PNL	.07 B, 0.23 Gd, 0.50 K, 0.15 Ce, 1.10 Ca	Flourite (Cubic)	HP	1700	10	9.3 (?)	Cubic HfO_2
$La_2Hf_2O_7$	PNL		Pyrochlore (Distorted Flouride)	HP	1700	10	8.0 (98%)	Pyrochlore (Distorted Flourite) + HfO_2
Pr_2Hf_2O7	PNL		Phrochlore (Distorted Flouride)	HP	1700	10	8.2 (98%)	
$SrZrO_3$	Cerac	0.03 Al, 0.23 B, 0.03 Cu, 0.1 Fe, 0.05 H_f 0.02 mg, 0.15 Si	Perovskite/Orthorhombic	HP	1700	10	5.6 (98%)	Orthorhombic $SrZrO_3$
Y_2O_3	PNL		C-Type R_2O_3 (Cubic)	HP	1650	10	5.2 (98%)	Cubic Y_2O_3
ZrO_2 $8Y_2O_3$	Ceramatec	6.0 Al (Mfg Analysis)	Flourite (Cubic)	--	--	--	5.51 (?)	Cubic ZrO_2
ZrO_2 $10Y_2O_3$	Cerac		Flourite (Cubic)	Sintered	1500	1200	5.99 (99%)	Cubic ZrO_2

(a) Hot Pressed

3.2 MATERIALS PREPARATION

High-density wafers nominally 19 mm (3/4 in.) in diameter and 1 mm (40 mils) in thickness were prepared from each oxide. Presintered rods of Al_2O_3, BeO, and $ZrO_2.8Y_2O_3$ were purchased commercially and sectioned with a diamond saw to obtain the desired wafer size specimens. Powders of $CaZrO_3$, $SrZrO_3$, and Y_2O_3 were purchased and then hot pressed to achieve wafers with densities approaching theoretical. The pyrochlore compounds and the yttria-stabilized ZrO_2 and H_fO_2 materials were made at the Pacific Northwest Laboratory (PNL) from soluble sulfates and chlorides dissolved in a hot sulfuric acid solution. Mixed solutions of the desired proportions were sprayed into an ammonium hydroxide solution to precipitate the compound. This precipitate was washed in a series of solvents, spray dried, and calcined. Wafers were made by hot pressing the resultant powders to densities near theoretical. All the hot pressing was preformed in graphite dies, in an argon atmosphere, and for the temperatures and times indicated in Table 3.1. The nominal pressing pressure was 34.5 MPa (5000 psi).

The principal elemental impurities for most of the materials measured by mass spectroscopy are also shown in Table 3.1. X-ray diffraction analysis was performed on several compounds; an automated stepping diffractometer was used to determine crystal structure. Densities were obtained by geometric measurement and then checked by water immersion. The geometrical measurements proved to be reasonably accurate since all samples had been pressed to a specific diameter and mechanically ground to close tolerances.

3.3 TEST SYSTEM

The experimental apparatus for measuring oxygen permeability is shown in Figure 3.1. Each test wafer was initially ground flat to facilitate a gas-tight seal. Platinum gaskets were effectively used to seal the wafers between the ends of spring-loaded alumina tubes. These 19-mm OD x 14.3-mm ID tubular sections provided the two opposing cells needed to impose an oxygen gradient across the test wafer. A close-fitting ring helped to prevent misalignment during assembly and testing, and an outer shroud tube helped to provide an

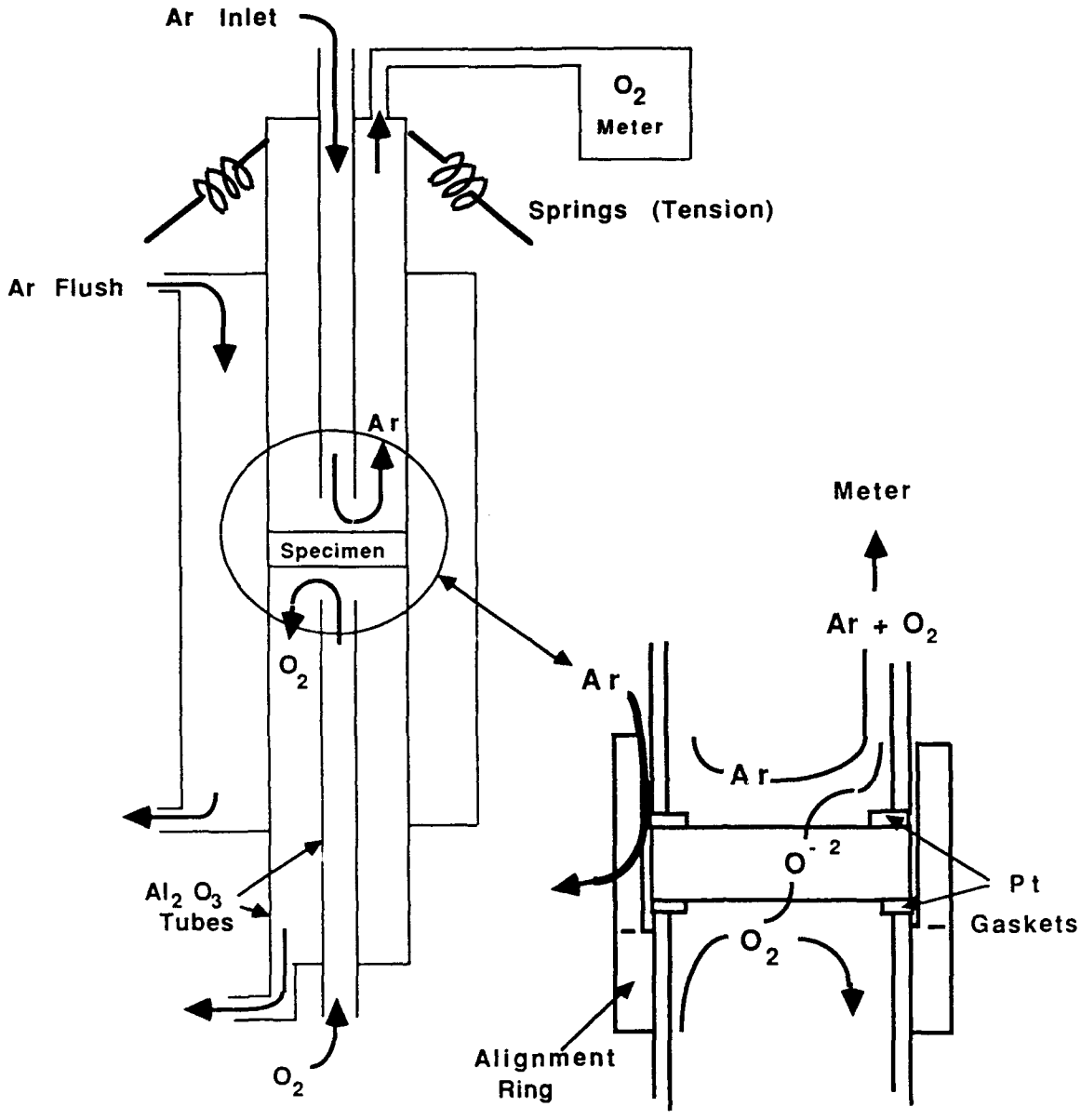

FIGURE 3.1. Schematic of Oxygen Permeability Apparatus

argon buffer zone and reduce oxygen diffusion or leakage from the furnace. This entire assembly was vertically positioned within a resistance-heated DelTech™ furnace.

High-purity argon (2 ppm O_2) was introduced to one side of the specimen through a smaller diameter tube positioned so that the gas flow could be

directed onto the surface (low oxygen side) of the test specimen. The gas with higher oxygen partial pressure, which consisted of air at one atmosphere pressure (0.21 atmospheres O_2), was supplied through a similar alumina tube on the opposite side of the test membrane. Oxygen that permeated the test membrane was swept up by the inert argon flow at 7.5 cc/s (1 SCFH) on the low-oxygen side and carried down stream to a Thermox™ (electrolytic cell) analyzer.

During initial heat-up, the spring-loaded assembly, alignment sleeve, and platinum gaskets prevented any cross leakage of oxygen between the two cells. High-purity argon was continuously flushed through the outer shroud to further minimize potential oxygen leakage.

3.4 MEASUREMENT PROCEDURE

During heat-up and equilibration, both upper and lower chambers were initially filled with the high purity (2 ppm O_2) argon. A measurement of oxygen partial pressure at the downstream solid electrolyte cell established a beginning reference for background oxygen. The lower chamber was then pressurized to 2 psi above atmospheric pressure to check integrity of the sample and the seals. A change in oxygen uptake at this point suggested that the sample was cracked or that a gas-tight seal had not yet formed. If this test was successful, air was introduced into the lower test cell. The increase in oxygen uptake at the downstream monitor connected to the upper cell indicated permeation. At steady state, the difference between the reference (background) and oxygen uptake at a given test temperature was used to calculate oxygen permeability.

Once equilibrium was achieved and a test value obtained, high-purity argon was reintroduced to displace the air in the lower cell, and a background or reference check was made on the upstream oxygen detector. After completing this step, air was again introduced to the lower cell and the measurement process repeated. This gave two measurements and a cross-check at each temperature.

The measurement process was typically started at 1100°C and repeated at 100°C increments up to a maximum temperature of 1700°C. At temperatures above

1700°C, the aluminum oxide cell tubes became distorted and oxygen leakage was sometimes observed. Under some conditions, this distortion was sufficient to break the seal and void the test. Once the measurements had been completed at 1700°C, the temperature was reduced in 100°C increments and the previous measurements verified.

An example of an oxygen permeability measurement plot for the $Pr_2Hf_2O_7$ composition as a function of temperature is shown in Figure 3.2. The lower curve represents the reference line with high-purity argon gas on both sides of the test sample. Note that the background level begins to increase above 1400°C as a result of oxygen leakage through the aluminum oxide cell walls. The upper curve represents the measurements taken when air is introduced into the lower side of the cell. The difference between the two curves is a measure of oxygen permeability through the material at a given temperature and oxygen gradient.

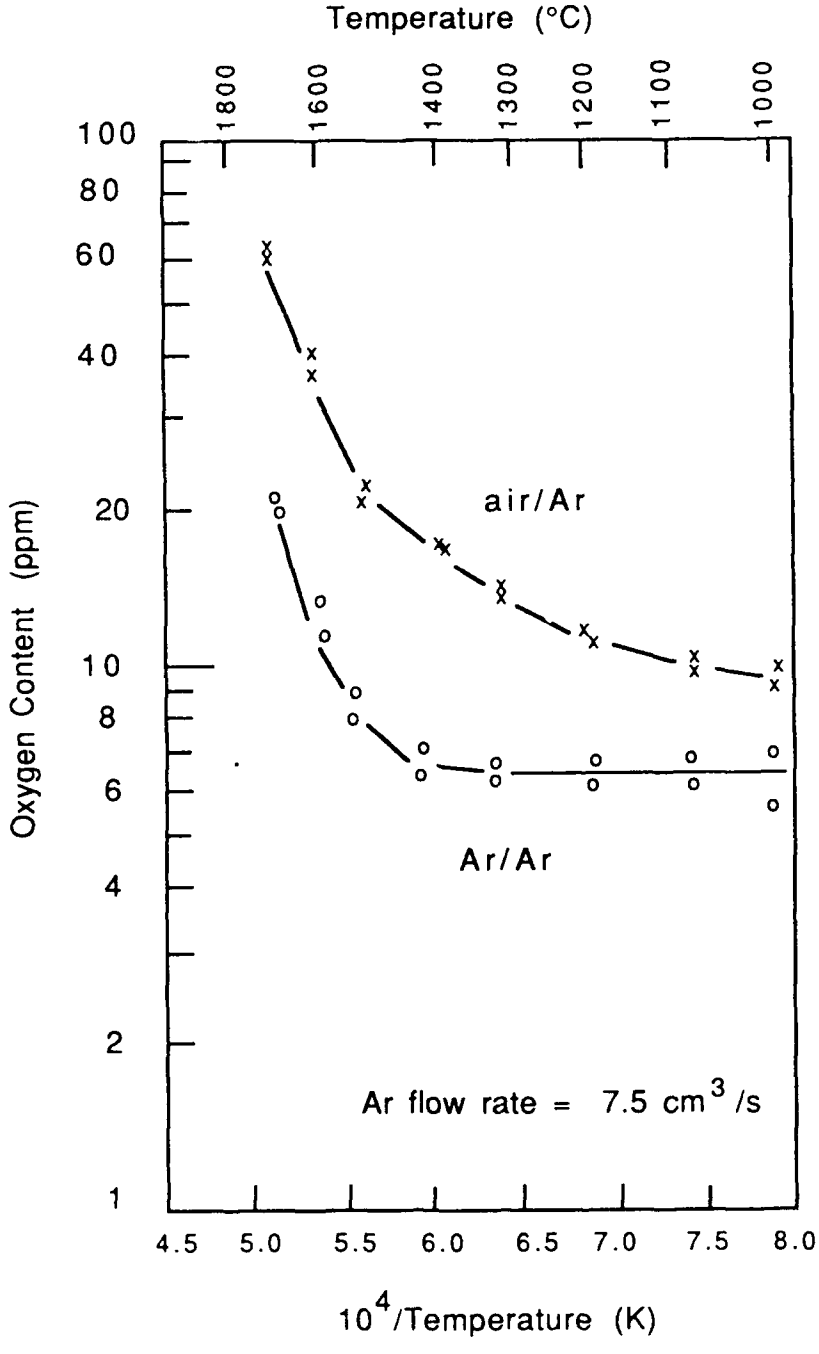

FIGURE 3.2. Experimental Measurements of Oxygen Permeability Through $Pr_2Hf_2O_7$

4.0 RESULTS

4.1 OXYGEN PERMEABILITY VERSUS TEMPERATURE

The temperature dependence of the oxygen permeability (constant) for each of the materials tested is shown in Figure 4.1. Each curve was derived from a plot similar to that shown in Figure 3.2. Equations for the temperature dependence of the permeability (constant) are listed in Table 4.1. As expected, the oxides with the lowest permeability to oxygen were those with the hexagonal close-packed crystal structure, e.g., alumina and beryllia. These two oxides exhibited permeabilities that were almost an order of magnitude lower than that of yttria at 1600°C and two orders of magnitude lower than the permeabilities of compound oxides with fluorite crystal structures. However, the temperature dependencies or activation energies, for alumina and beryllia were greater than for yttria. At temperatures approaching 1800°C (extrapolated), yttria may have the lowest permeability to oxygen. Data for the hexagonal close-packed oxides, e.g., Al_2O_3, BeO, and Y_2O_3, were not obtained below 1500°C because the differential oxygen pressure was very small and the measurement uncertainty was too large.

Lanthanum hafnate had the lowest permeability of the compound oxides up to about 1500°C. Above 1500°C, calcium zirconate exhibited the lowest permeability. The activation energy for $La_2Hf_2O_7$ was higher than $CaZrO_3$ suggesting that a different diffusion mechanism may be operable. As expected, oxides with fluorite lattice structures, e.g., HfO_2 and ZrO_2 stabilized with yttria, exhibited the highest permeability to oxygen of all the materials tested.

4.2 BENCHMARK COMPARISONS

The permeability values obtained for alumina were compared to those reported by Volk and Mezaros [3] and are shown in Figure 4.2. Very good agreement is observed over the temperature range where comparisons are valid. Comparisons were also made for yttria and yttria-stabilized zirconia against values calculated from electrical conductivity measurements. The equation needed for thiscalculation was previously established by Kroger [4]:

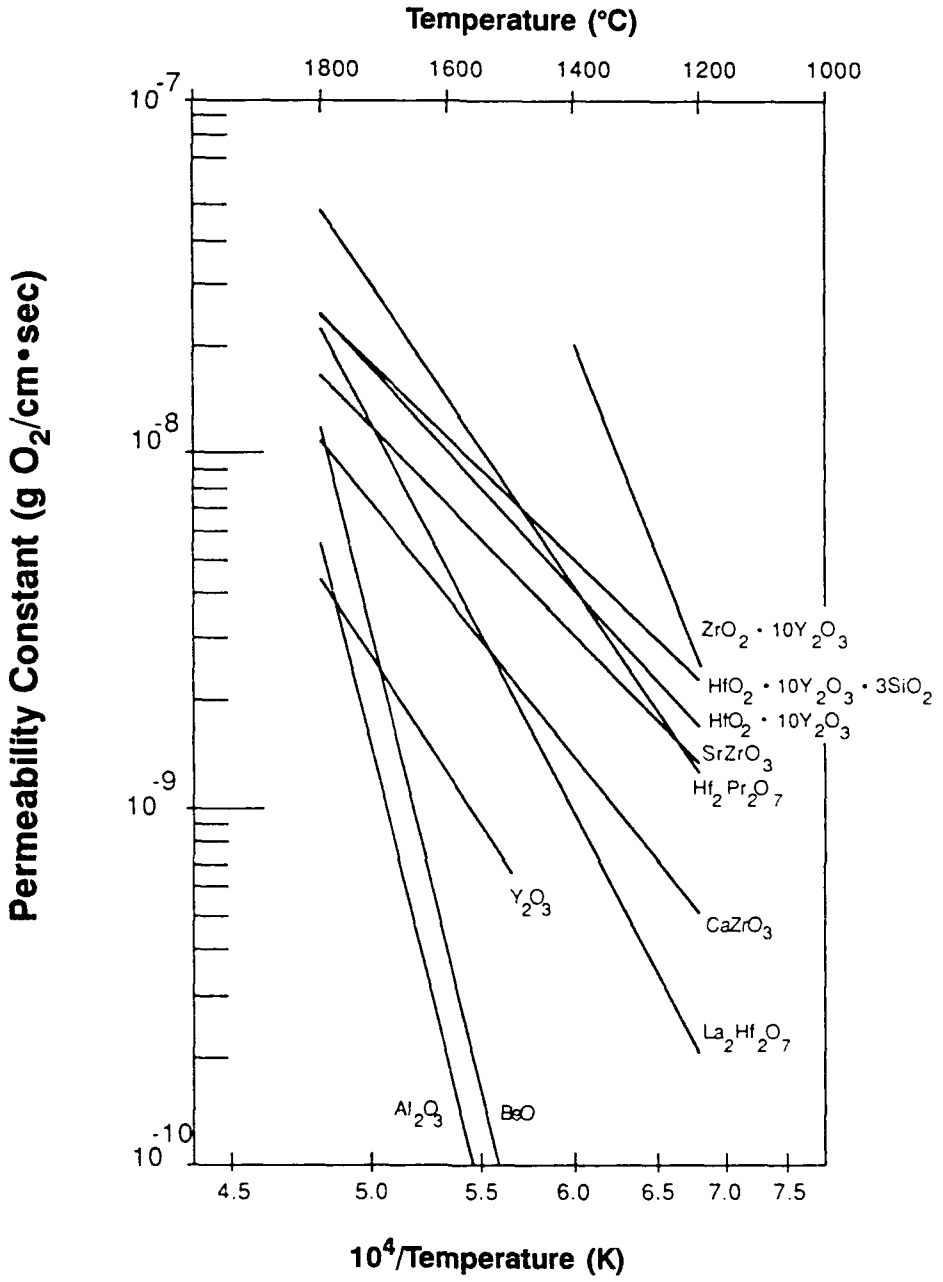

FIGURE 4.1. Temperature Dependence of Permeability Constants at 0.21 atm Oxygen Partial Pressure

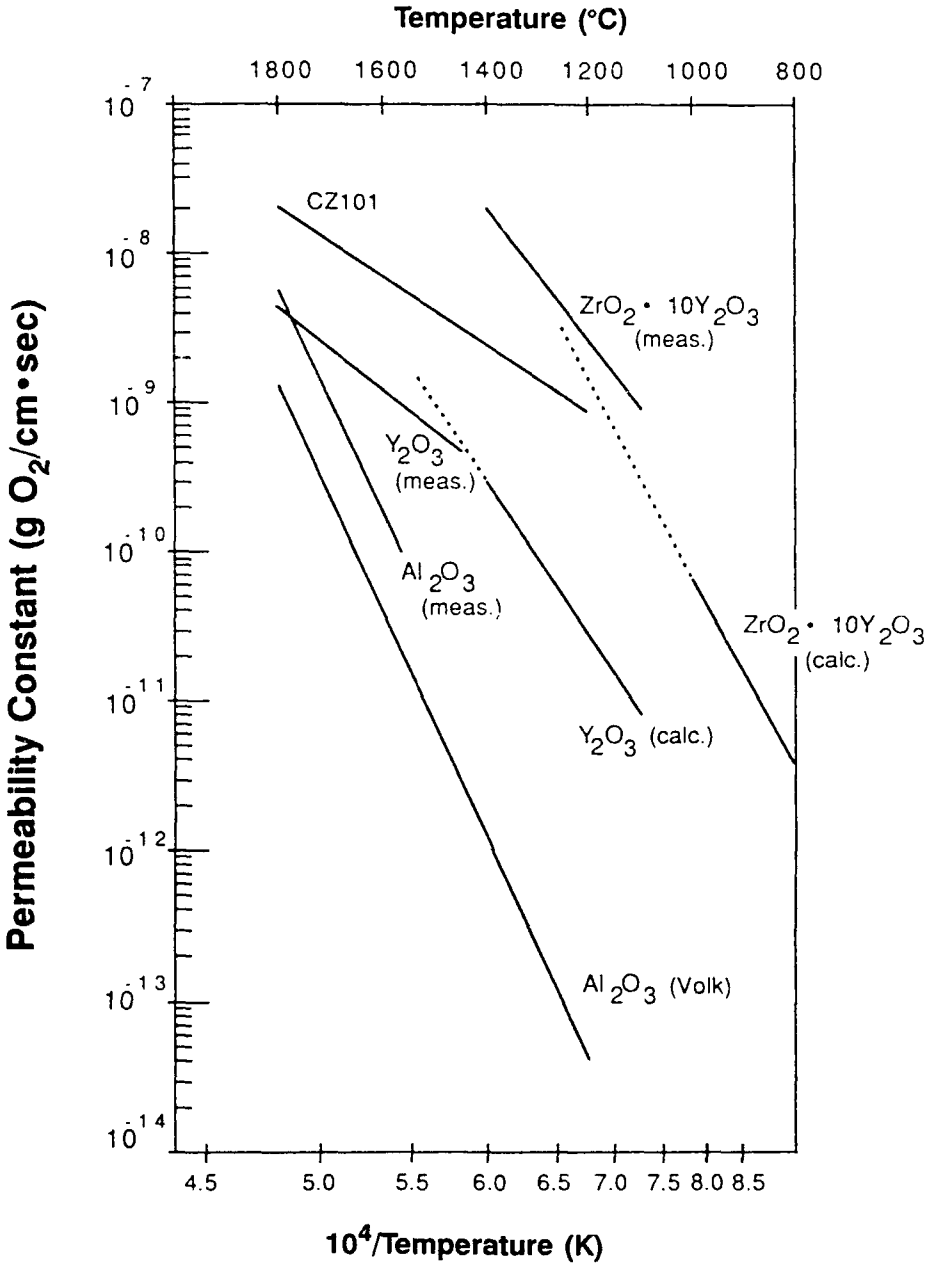

FIGURE 4.2 Comparison of Permeability Constants for ZrO_2 $10Y_2O_3$, and Y_2O_3 with Calculated Values

TABLE 4.1. Permeability Constants for Selected Oxides

Material	Permeability Constant (p•l) g O_2/cm
$ZrO_2 \cdot 10Y_2O_3$	$3.50 \times 10^{-2} e^{\frac{-23,960}{T(°K)}}$
$CaZrO_3$	$2.05 \times 10^{-5} e^{\frac{-15,420}{T(°K)}}$
$HfO_2 \cdot 10Y_2O_3$	$1.93 \times 10^{-5} e^{\frac{-13,760}{T(°K)}}$
$HfO_2 \cdot 10Y_2O_3 \cdot 3SiO_2$	$8.56 \times 10^{-6} e^{\frac{-12,100}{T(°K)}}$
$Hf_2Pr_2O_7$	$3.88 \times 10^{-4} e^{\frac{-18,590}{T(°K)}}$
$SrZrO_3$	$8.56 \times 10^{-6} e^{\frac{-12,910}{T(°K)}}$
$La_2Hf_2O_7$	$2.25 \times 10^{-3} e^{\frac{-23,850}{T(°K)}}$
Y_2O_3	$4.72 \times 10^{-5} e^{\frac{19,230}{T(°K)}}$
BeO	$3.38 \times 10_3 e^{\frac{-54,640}{T(°K)}}$
Al_2O_3	$1.21 \times 10^3 e^{\frac{-54,080}{T(°K)}}$
CZ101	$4.55 \times 10^{-5} e^{\frac{-16,150}{T(°K)}}$

$$P \cdot x = JO_{2 \cdot x} = \frac{Kt}{8e_2} \int_{PO_2^I}^{PO_2^{II}} \cdot ti \; d \ln PO_2 \qquad (3)$$

The electronic and ionic transference numbers, t_e, and t_i must be known along with the total electrical conductivity (σ). In general, all three parameters are functions of oxygen concentration.

For yttria, σ, te, and ti were obtained from the work of Norby and Kofstad [5]. Appropriate values for yttria-stabilized zirconia were taken from the work of Burke et al. [6]. Comparisons are shown in Figure 4.2 and reasonable agreement is again observed. These calculations represent a lower bound for oxygen permeability since they are based on particle conductivities in a homogeneous medium, and do not include contributions from short circuit pathways such as grain boundaries or from the diffusion of molecular oxygen. Experimental permeability measurements are expected to exhibit higher values than calculations based on electrical conductivity data.

A comparison of yttria-stabilized zirconia and Hafnia in Figure 4.1 indicates that zirconia may have a higher permeability and perhaps a higher activation energy than hafnia. These results contradict the work of Smith, Metaros, and Amata [7], who reported similar activation energies for calcium-stabilized zirconia and hafnia. If the defects and defect concentrations were similar, the activation energies should also be similar unless large differences in impurity levels were present. The reason for the differences reported herein are not presently explained and may reflect some experimental variability.

4.3 POROSITY EFFECTS

One set of yttria-stabilized zirconia samples were prepared to examine the effects of porosity on oxygen permeability. A small quantity of 10% yttria-stabilized zirconia powder was premixed by ball milling with 8 to 40 μm particle size polyethylene powder. Pellets were then pressed and sintered to 1600°C for 20 h. The resultant porosity was approximately 10% as determined by micrographic examination. The porosity was mostly spherical but was not uniformly distributed on a macroscopic scale (see Figure 4.3). A comparison of immersion and geometrical measured densities indicated that the porosity was closed and not open to the surface. This conclusion is also supported by the micrographs.

A comparison of the temperature dependence for the two oxygen permeability curves is shown in Figure 4.4. Calculated values obtained from electrical conductivity measurements are also included. There is almost an order-of-magnitude difference in oxygen permeability at 1100°C, but at higher

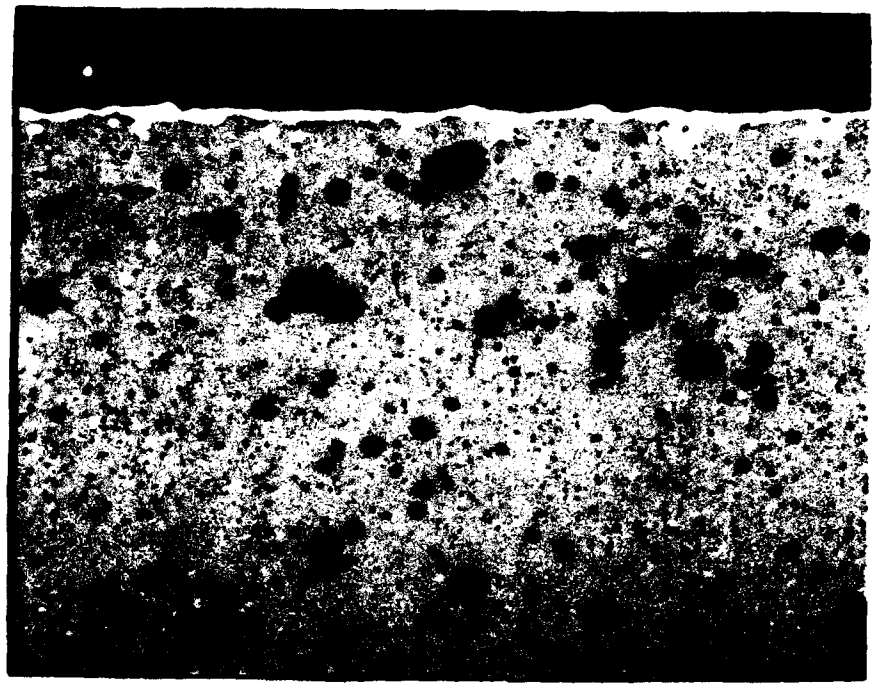

A $p = 5.34$ gms/cc
$p \cdot l = 5.61 \times 10^{-8}$ gms O_2/cm•sec

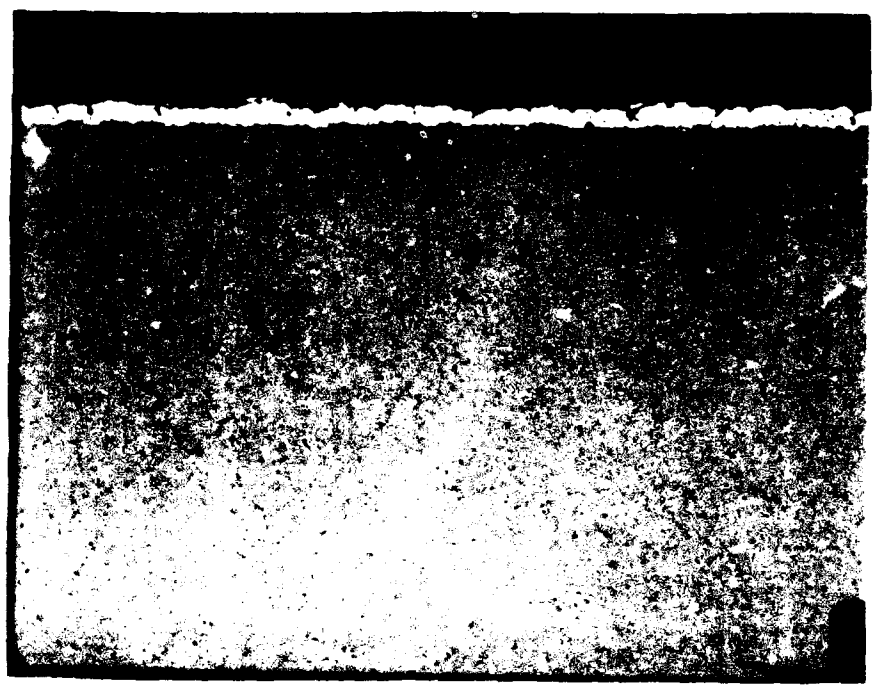

B $p = 5.95$ gms/cc
$p \cdot l = 2 \times 10^{-8}$ gms O_2/cm•sec

FIGURE 4.3. Optical Micrographs of $ZrO_2 \cdot 10Y_2O_3$. Permeability measurements were at 1400°C.

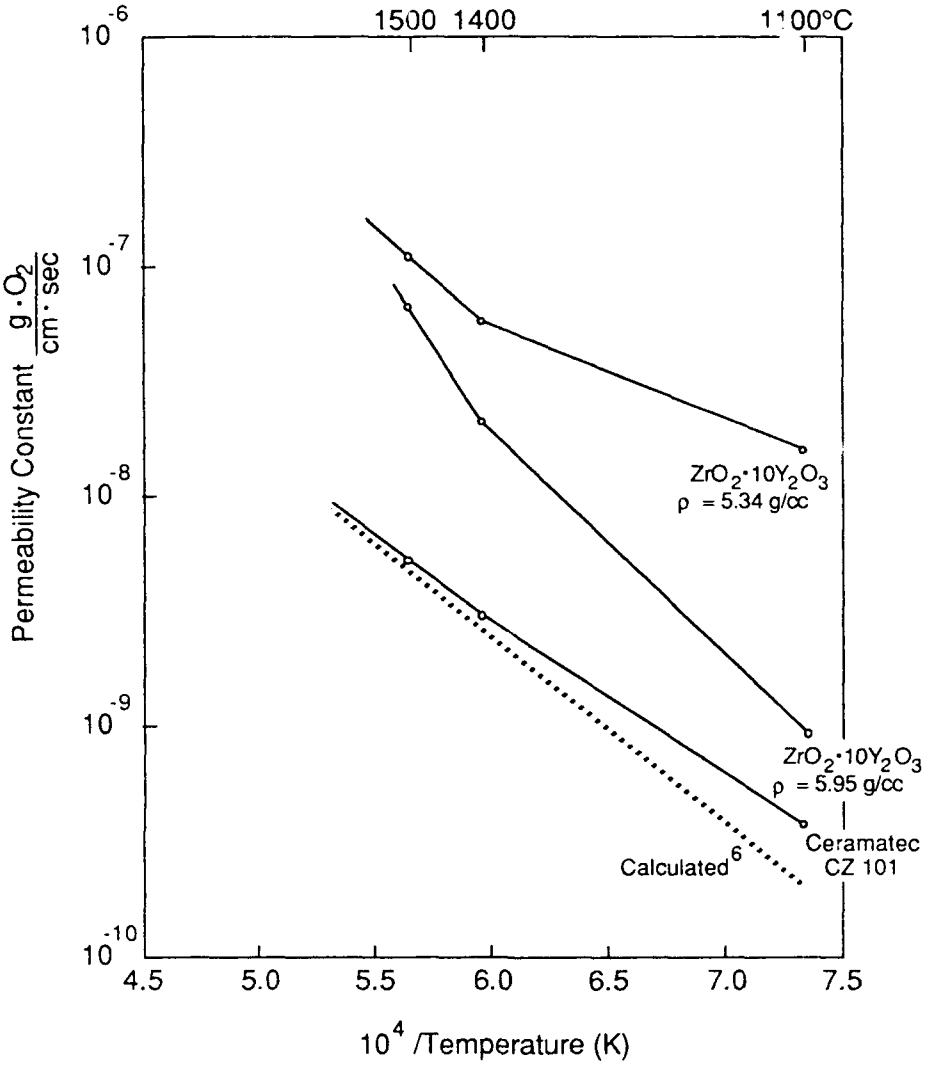

FIGURE 4.4. Temperature Dependence of Oxygen Permeability Constant for $ZrO_2 \cdot 10Y_2O_3$ of Different Density 0.21 atm at Oxygen Partial Pressure

temperatures, the two curves converge. The high-density sample exhibits two to three times the permeability of the lower density sample at 1400°C. The experimental data for these two samples were not obtained in the usual 100°C increments, and the reason for the change in slope between 1400 and 1500°C is not entirely clear. Although this type behavior is often explained on the basis of change in mechanism from impurity controlled to intrinsic diffusion at high temperatures, a stabilized zirconia would not be expected to exhibit such a trend because of the high concentration of vacancy defects. It is more

likely that the accuracy of the permeability measurements at the lower 1100°C temperature are uncertain since the difference in oxygen measurements between the reference and test case is very small at the lower temperature.

An interesting result was the relatively low permeability exhibited by the Ceramatec, CZ101, material, which was very close to the calculated value. The theoretical density of this sample was not known because it contained 6 and 7 wt% aluminum for a sintering aid. Optical metallography, see Figure 4.5, indicates that the porosity is about ten percent. The presence of the small amount of aluminum apparently reduces the permeability despite the lower density.

4.4 SEGREGATION IN AN OXYGEN GRADIENT

The typical oxygen partial pressure gradient used in these tests varied from 0.21 atmospheres on one side of the test sample to approximately 2×10^{-6} atmospheres on the other side. It has been shown by Laqua and Schmalzried [8] that demixing can occur in a mixed oxide if there are significant differences in the cation diffusion rates. Several of the test samples were subjected to energy dispersive x-ray analysis following the permeability experiments to determine if cation segregation had occurred. These results are shown in Figure 4.6. Various degrees of segregation were observed ranging from almost complete partitioning of the strontium zirconate $SrZrO_3$ sample to almost no segregation in the case of lanthanum hafnate $La_2Hf_2O_7$.

This demixing phenomenon could easily occur in any situation where compound oxides are subjected to oxygen chemical potential gradients; it is therefore an important concern in the application of multicomponent ceramics at high temperatures. If a stable ternary oxide ABO_x is subjected to an oxygen potential gradient, demixing occurs if the diffusion coefficient $D_a > D_b$ is $>> D_o$. Under these conditions, the crystal will normally be enriched in AO at the side of higher oxygen potential [8]. The ratio of oxygen partial pressures necessary to kinetically decompose a mixed oxide compound will, in general, be inversely proportional to the ratio of the cation diffusivities.

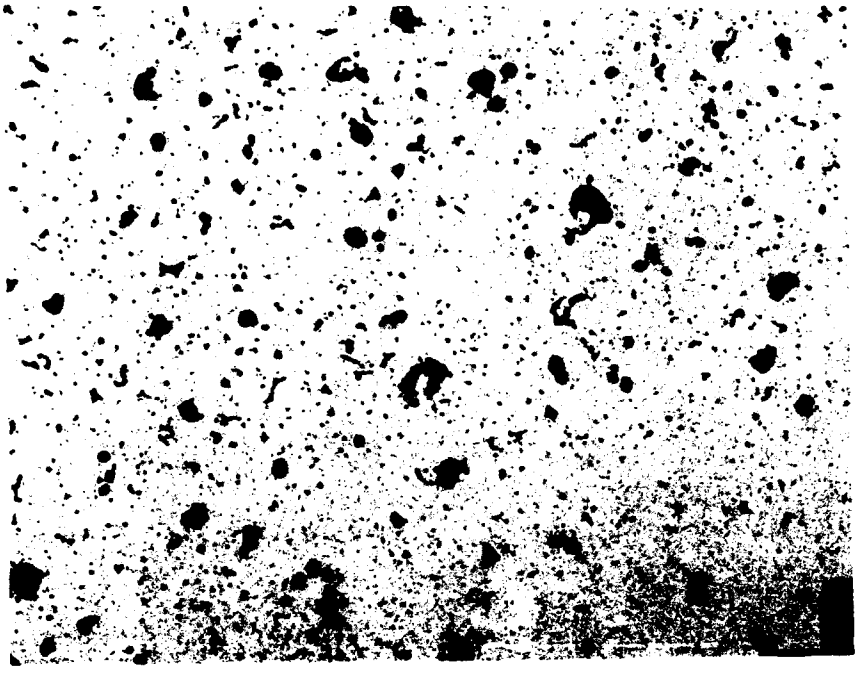

250X

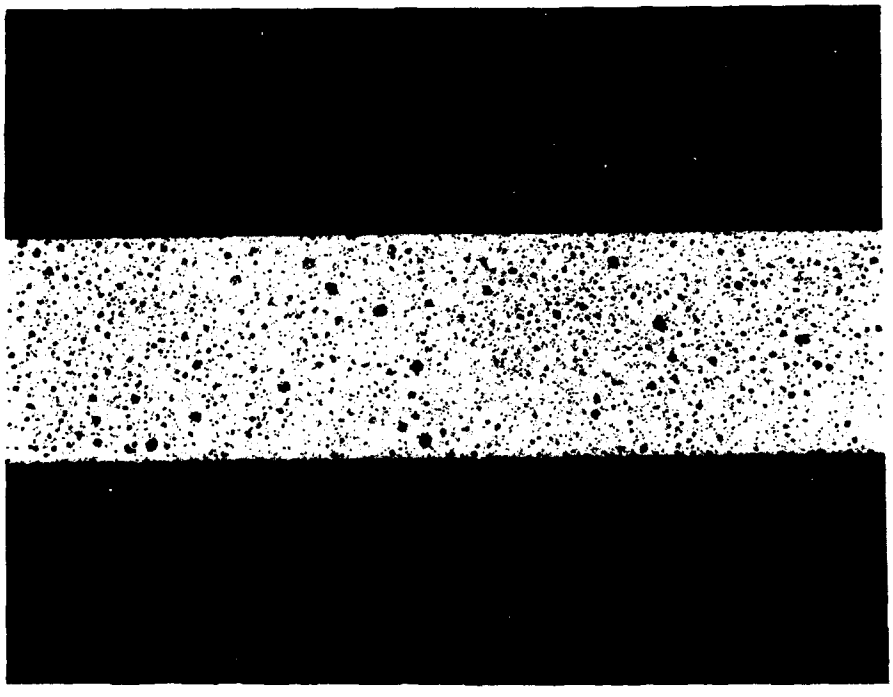

31X

FIGURE 4.5. Optical Micrograph of CZ101* Stabilized Zirconia.
*Product of Ceramatec.

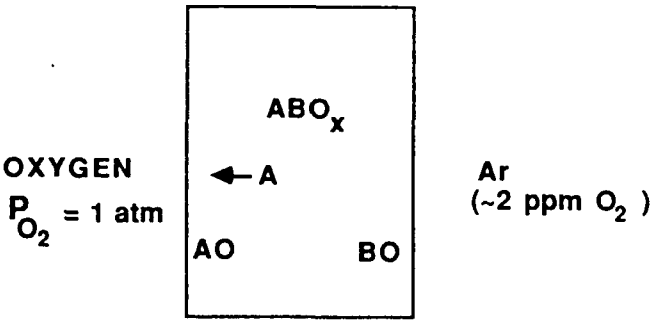

OXIDE		COMPOSITION			% ENRICHMENT
		INITIAL	FINAL (AIR SIDE)	FINAL (Ar SIDE)	
$SrZrO_3$	A	Sr: 50	Sr: 100	Sr: 0	100
	B	Zr: 50	Zr: 0	Zr: 100	
$Pr_2Hf_2O_7$	A	Pr: 50	Pr: 60	Pr: 40	20
	B	Hf: 50	Hf: 40	Hf: 60	
HfO_2-Y_2O_3	A	Y: 10	Y: 11	Y: 9	10
	B	Hf: 90	Hf: 89	Hf: 91	
$La_2Hf_2O_7$	A	La: 50	La: 50.5	La: 49.5	1
	B	Hf: 50	Hf: 49.5	Hf: 50.5	

FIGURE 4.6. Segregation in an Oxygen Gradient

5.0 DISCUSSION

The surfaces of oxidation-sensitive structural components must be protected from degradation over the projected lifetime of the component, otherwise integrity will be lost. For extended life applications, coatings or barriers must have oxygen permeabilities on the order of 10^{-10} to 10^{-12} g O_2/cm s. The oxide systems with lowest oxygen permeabilities measured in these studies were Al_2O_3 and BeO, but even these would not provide sufficient protection at temperatures above 1500°C. All other oxide systems studied in this work appear to have unacceptable oxygen diffusion rates.

Comparisons with other materials, including silica and the noble metals Ir and Rh, are shown in Figure 5.1. The SiO_2 curve was calculated from Motzfeldt's [9] data compilation derived from oxide scales that had been thermally grown on silicon carbide and silicon nitride. In silica, diffusion of oxygen reportedly [9-11] occurs by transport of molecular species as opposed to ionic oxygen, and the oxygen permeability is considerably lower than for the oxide systems reported herein. This fact has also been demonstrated by the successful application of silicon carbide and silicon nitride coatings for protecting carbon/carbon composites and by the commercial use of molydisilicide heating elements. Silica forming layers will even protect carbon/carbon to temperatures as high as 1700°C for a few hours [12-13].

There is some disagreement over the mechanism of oxygen diffusion in silica. Norton [14] determined the permeation of oxygen through a silica membrane in the temperature range between 950 and 1080°C at oxygen pressures from 300 to 800 torr. Williams [15] measured oxygen diffusion by a tracer uptake in silica fibers. Both researchers noted that the permeability varied linearly with oxygen partial pressure and concluded that molecular oxygen was responsible for the transport. Sucov [16] also studied the diffusivity of oxygen using isotopic tracers in silica fibers, but proposed that the oxygen transport mechanism was controlled by vacancies. More recently, Boyce [10] utilized double oxidation techniques where oxidation is performed in an atmosphere containing one isotope of oxygen followed by oxidation in an atmosphere containing a second isotope. The techniques yield complex tracer concentration profiles that can be explained only on the basis of mechanisms

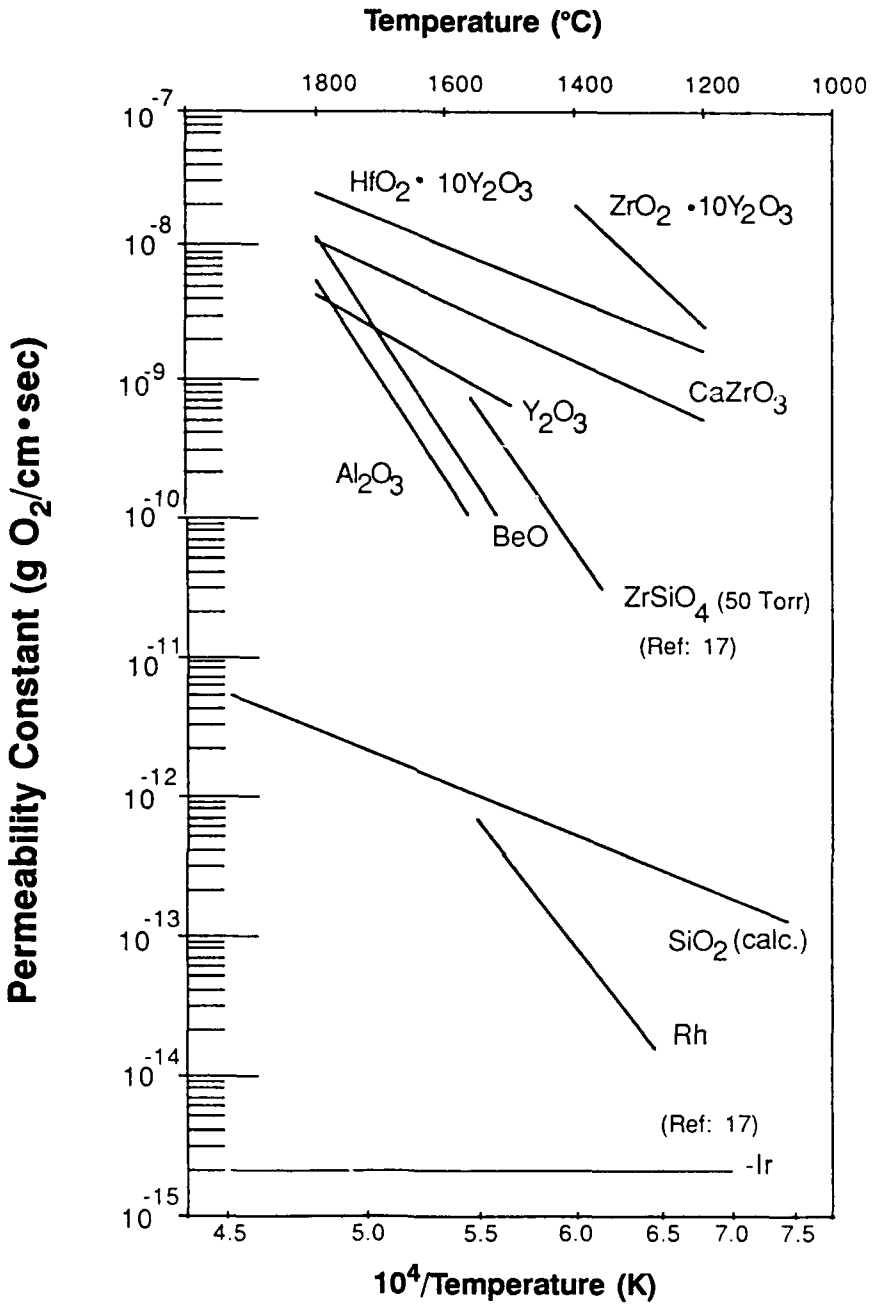

FIGURE 5.1. Range of Oxygen Permeability Through Several Oxides and Noble Metals at 0.21 atm Oxygen Partial Pressure

involving surface and network-interstitial exchange with the primary transport process occurring by diffusion of molecular species.

The fact that silica exhibits the lowest permeability to oxygen may lead to the conclusion that the refractory silicates could also be candidate materials for coating systems. The principal silicates of interest would likely include zirconium silicate ($ZrSiO_4$), hafnium silicate ($HfSiO_4$), or thorium silicate ($ThSiO_4$). Some data for zirconium silicate was reported in the work of Criscione [17] et al., and the permeability constant as a function of temperature at an oxygen pressure of 50 torr is included in Figure 5.1. This curve was obtained at a lower oxygen pressure than was present for other oxides; however, the permeability appears to be comparable to that of beryllia.

6.0 CONCLUSIONS

Although the hexagonal close-packed oxides of beryllia, alumina, and yttria exhibit the lowest permeability to oxygen of the refractory oxides, they do not appear to be useful as oxygen protection barriers at temperatures above 1500°C. If the results are extrapolated to temperatures above 1700°C, yttria appears to have the lowest permeability.

Silica may be the only refractory ceramic oxide with an acceptably low permeability of oxygen over a wide temperature range. This fact has already been demonstrated through the success of silicon carbide coated carbon/carbon and molydisilicide heating elements, which function at elevated temperatures for extended periods of time in oxidizing environments. Although compound silicates were not studied in this work, it is questionable if they would exhibit a lower permeability to oxygen than pure silica.

Compound oxides will segregate in an oxygen gradient if their respective cation diffusivities are different. This is an important consideration in the use of mixed oxides in composite systems.

7.0 REFERENCES

1. E. E. Hermes and R. J. Kerans, "Degradation of Nonoxide Reinforcements and Oxide Matrix Composites," MRS Symposium, Materials Stability and Environmental Degradation, Vol 125 (1988).

2. W. D. Kingery, H. K. Bowen, and D. E. Uhlman, Introduction to Ceramics, John Wiley and Sons, New York, pp. 217-263 (1976).

3. H. F. Volk and F. W. Mezaros, "Oxygen Permeation Through Alumina - Influence of Micro Structures and Purity," Chapter 30 in Ceramic Micro Structures, R. M. Fullrath and J. A. Pask, ed., John Wiley and Sons, New York, (1968).

4. F. A. Kroger, The Chemistry of Imperfect Crystals, North Holland Publishing Co., John Wiley and Sons, New York (1964).

5. T. Norby and P. Kofstad, "Electrical Conductivity of Y_2O_3 as a Function of Oxygen Partial Pressure in Wet and Dry Atmospheres," Journal American Ceramic Society, 69 (11) 784-89 (1986).

6. L. D. Burke, H. Richert, and R. Sterner, Z Phys Chem NF, 74, 146 (1971).

7. A. W. Smith, F. W. Mezaros, and C. D. Amata, "Permeability of Zirconia, Hafnia, and Thoria to Oxygen," Journal of the American Ceramic Society, 49 (5), 240-244 (1966).

8. W. Laqua and H. Schmalzried, "Multi Component Oxides in Oxygen Potential Gradients," High Temperature Corrosion, NACE-6, R.A. Rapp, ed., 115-120 (1983).

9. K. Motzfeldt, "On the Rates of Oxidation of Silicon and of Silicon Carbide and Oxygen in Correlation with Permeability of Silica Glass," Acta Chemica Scandinavia, 18 (7), 1596-1606 (1964).

10. R. Boyce, MS Thesis, "The Mechanisms of Oxygen Transport in Vitreous Silica," The Ohio State University (1985).

11. A. S. Sherman, MS Thesis, "Oyxgen Transport and Electronic Conduction in Fused Silica and Thermally Grown Silicon Dioxide," The Ohio State University (1987).

12. J. R. Strife and J. E. Sheehan, "Ceramic Coatings for Carbon-Carbon Composites," Ceramic Bulletin, 67 (2) 369-374 (1988).

13. J. R. Strife. "Development of High Temperature Oxidation Protection for Carbon/Carbon Composites," R87-916789-12 (1987).

14. F. J. Norton, "Permeability of Gaseous Oxygen Through Vitreous Silica," Nature, 191, 701 (1961).

15. E. L. Williams, "Diffusion of Oxygen in Fused Silica," Journal American Ceramic Society, 48, 190-194 (1965).

16. E. W. Sucov, "Diffusion of Oxygen in Vitreous Silica," Journal American Ceramic Society, 46, 14-20 (1963).

17. J. M. Criscione et al., "High Temperature Protective Coatings for Graphite," ML-TDR-64-173, Part III (1965).

☆U.S. GOVERNMENT PRINTING OFFICE: 1992 - 648-127/62169